Electron Acceleration by a Transverse Electromagnetic Wave Supplemented with a Crossed Static Magnetic Field

Noboru Yugami, Kazuo Kikuta, and Yasushi Nishida

Department of Electrical and Electronic Engineering, Utsunomiya University, 2753 Ishii-machi, Utsunomiya, Tochigi 321, Japan

(Received 7 June 1994)

An electron linear accelerator has been demonstrated that uses a slow transverse electromagnetic wave (TE wave, 10 kW) supplemented with a crossed static magnetic field. An initial energy gain of 6.0 keV for electrons is observed from an incident energy of 62 keV in a 0.5 m accelerator without an additional external magnetic field. When an external vertical magnetic field of 2.5 G is applied under the same conditions, an additional 7.5 keV energy gain is observed. The results show the feasibility of making a compact accelerator using TE mode electromagnetic waves.

PACS numbers: 29.17.+w, 41.75.Di, 52.75.Di

Recent interest in charged particle accelerators has focused on generating much higher acceleration gradients than is possible in the present conventional accelerators, which have typical acceleration gradients of about 10–20 MeV/m. In the last decade new acceleration schemes, with much higher acceleration gradients, have been proposed and demonstrated in proof-of-principle experiments [1–13], e.g., the plasma wake field accelerator (PWFA), the plasma beat wave accelerator (PBWA), and the $v_p \times B_0$ accelerator or surfatron, where v_p is the wave phase velocity and B_0 is the applied static magnetic field. The possibility of charged particle acceleration using a transverse electric field supplemented with a weak, external, static magnetic field parallel to the wave magnetic field has also been discussed [14,15].

$v_p \times B_0$ acceleration phenomena [6–8,10], in which a static magnetic field is applied perpendicular to the wave propagation direction and the particles are accelerated continuously along the wave front at constant phase with respect to the wave until the trapping condition breaks, have been observed in microwave-plasma interaction experiments [8,9]. With this mechanism the presence of a plasma is not essential, so the charged particles can be accelerated even in a vacuum [11,12].

In the $v_p \times B_0$ scheme, the theory indicates that electron acceleration can be realized even in a transverse electromagnetic wave mode (TE wave). This Letter reports, to the best of our knowledge, the first results of proof-of-principle experiments on the $v_p \times B_0$ acceleration scheme with a TE wave in a vacuum waveguide [14,15]. The results show the feasibility of making high gradient compact accelerators.

Takeuchi *et al.* [14] originally proposed the TE-mode accelerator using dielectric materials and investigated the stability of the particle orbit in the wave frame. This theory shows that a transverse electromagnetic wave propagating through the slow wave structure can trap and accelerate charged particles.

It is convenient to review the acceleration mechanism briefly. Suppose that a transverse electromagnetic wave which has the maximum electric field E_x and the maximum magnetic field B_y in the x and y directions, respectively, propagates with the phase velocity v_p in the z direction (see Fig. 1). When an external static magnetic field B_0, less than B_y, is applied in the y direction, there exist two magnetic neutral points A and B where the electric fields are nonzero. Around point B, the Lorentz force acts on the particles, and bunches them in the z direction. However, particles staying exactly at point A or B are accelerated continuously in the x direction by the wave electric field if $v_p \approx v$, the particle velocity. Therefore the particles are bunched around point B and accelerated in the x direction in the x-z plane.

The trapping condition in a wave trough in this scheme is obtained by balancing the force in the wave propagation direction (z direction) such that [14]

$$|B_y| > \gamma_p^2 B_0 , \tag{1}$$

where $\gamma_p = \{1 - (v_p/c)^2\}^{-1/2}$ is the Lorentz factor measured with the wave phase velocity v_p. When Eq. (1) is satisfied, the electron can be accelerated continuously without detrapping from the wave trough. Now we can obtain the energy gain $d\gamma/dz$ of the trapped particles in steady state for unit length in the laboratory frame,

$$\frac{d\gamma}{dz} = \frac{q\gamma_p^2 B_0}{mc^2} v_x . \tag{2}$$

In this scheme, a charged particle with a velocity of almost the speed of light can interact with the electromagnetic wave in vacuum.

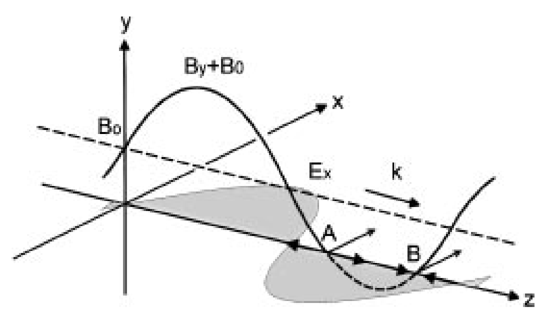

FIG. 1. Schematic diagram for $v_p \times B$ acceleration scheme using the TE mode.

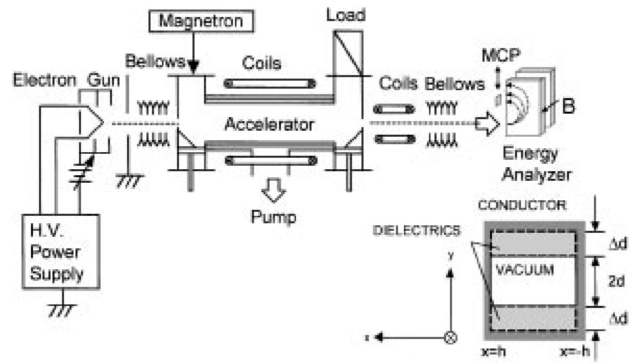

FIG. 2. Experimental apparatus. The inset shows the cross sectional view of the dielectric loaded waveguide.

A schematic view of the experimental setup is shown in Fig. 2, and the cross section of the slow-wave structure employed here is shown in the inset of Fig. 2. Because of the slow injection beam energy in the present facility, the slow-wave structure must be employed. The dimensions of the slow wave structure are listed in Table I.

The injected electron beam is initially accelerated by a high-voltage dc power supply with a maximum energy of up to 100 keV and current of 1 mA. Here we used a Pierce-type gun with a hair-pin-type cathode.

The electrons accelerated through the accelerator are analyzed by a magnetic-field-bending type of energy analyzer. The electrons are detected by a microchannel plate (MCP) electron multiplier with a 2-mm slit in front of it. The MCP is scanned spatially in the analyzer; the position at which the signal is detected corresponds to the energy, and the signal intensities to the electron fluxes. The maximum resolution of the energy analyzer is less than 0.1 keV. This instrument is calibrated with the abovementioned electron beam source. The calibration is carried out by changing the acceleration voltages without rf power before and after the experiments. When the electron energy is measured, the energy analyzer is adjusted such that the electrons are injected normal to its inlet slit.

A pulsed electromagnetic wave of maximum power 10 kW is generated by a magnetron with a typical pulse width of 5 μs and repetition rate of 10 Hz. The generated microwaves are absorbed by a nonreflecting dummy load after going through the slow-wave structure in the accelerator main body. The electric field intensity is expected to be about 20–30 kV/m, but experimentally it is estimated to be about 30–40 kV/m (shown later).

TABLE I. Dimensions of the dielectric wave guide.

Dielectric materials	Macorl	Folsteright
Dielectric constant	5.68	7.0
	(f = 8.6 GHz)	(f = 1 MHz)
Accelerator length	48 cm	
Thickness Δd	50 mm	
Width $2h$	50 mm	
Separation $2d$	13–33 mm	
Height	113–133 mm	
$\ell(= 2d + 2\Delta d)$		

The static, vertical magnetic field for $v_p \times B_0$ acceleration is generated by a pair of saddle-shaped external coils. Uniformity less than 3% covers a length of 32 cm (40 cm for 5%) in the z direction and 5 cm in the x and y directions. A maximum field strength of 10 G is measured at the center axis of the accelerator. This value should be large enough to demonstrate the $v_p \times B_0$ accelerator principle with a TE mode under the present experimental parameters. The whole vacuum system is pumped out below 5×10^{-7} Torr by a turbomolecular pump.

Before the main acceleration experiments were performed, the phase velocity in the waveguide was measured by the interferometry method. Although the theory predicts the phase velocity, determined by the geometry of the waveguide and the dielectric constant, a precise velocity should be measured, because the dielectric constant is unknown in such a high-frequency regime. We employed a low power rf source for this purpose and a small probe (1 mm length $\times$ 0.2 mm diameter) was used for picking up the rf signal in the slow-wave structure. A typical experimental result for the phase velocity v_p is shown in Fig. 3. Here an example of the interferometic wave form is shown in the inset. We tried many times, and the average result is marked by the solid circle in Fig. 3. In this figure, the solid line denoted "Th." is the theoretical result obtained from the dispersion relation in the slow-wave structure, after fitting it to the experiment at $\Delta d/d = 7.5$, giving a relative dielectric constant of 5.65. Using this value, we have designed the slow-wave structure with a phase velocity of $0.46c$ (corresponding to an energy of 65 keV) at $\Delta d/d = 3.0$, shown in Fig. 3.

When the present machine performs as an accelerator without the static magnetic field, resonantly accelerated electrons are observed; a typical example is shown in Fig. 4. A maximum energy increment of $\Delta\varepsilon_0 = \varepsilon - \varepsilon_{\mathrm{in}} = 6.0$ keV, where ε is the final electron energy and $\varepsilon_{\mathrm{in}}$ the incident electron energy, is observed when $\varepsilon_{\mathrm{in}} = 62$ keV. This implies that this slow-wave structure

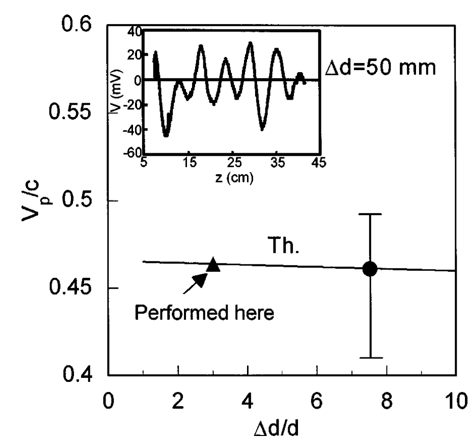

FIG. 3. Experimental and calculated results of phase velocity vs the distance d. An arrow shows the condition employed for the present acceleration experiments. "Th." shows the calculated phase velocity. The inset shows an example of the interferometer output of the phase measurement.

resonates with energy 62 keV at the rf frequency 2.45 GHz. The vertical error bars indicate the variation in the electron energy resulting from the instability of beam transparency through the waveguide. The solid line was calculated theoretically after adjusting the resonance energy to 62 keV, which is different from the designed value of 65 keV. This apparent disagreement of the resonance energy may be because efficient acceleration is realized when the wave phase velocity is slightly larger than the beam velocity. When the wave phase velocity is less than the beam velocity, strong deceleration of particles occurs. At $\varepsilon_{\rm in} \geq 64$ keV, no acceleration or even deceleration of particle energy is observed. The calculated curve in Fig. 4 does not include these effects; it just shows the resonance characteristics of the slow-wave structure. These results indicate that a dielectric slow-wave structure can work as an electron accelerator with a pure transverse electromagnetic wave propagating with a phase velocity slightly larger than the electron beam velocity.

Typical examples of the electron energy spectra observed when a vertical magnetic field is applied with an incident electron energy of 62 keV are shown in Fig. 5. The arrows indicate the peak electron fluxes where energy is measured. When the static magnetic field is increased, the electron energy increases until $B_0 = 2$ G in this figure. With further increase of the magnetic field ($B_0 > 2$ G), no further acceleration occurs, as the trapping condition for the particles [Eq. (1)] is violated. When a vertical magnetic field is applied, both accelerated and a small number of decelerated particles are observed, as seen in the figure, although we are interested in the accelerated particles. In our present apparatus, the electron beam is injected continuously (in dc). This means that some particles may have a chance to be thrown into the deceleration phase at first and then shifted to the acceleration phase eventually. In order to improve these characteristics, electrons could be thrown into the acceleration phase by using a pulsed electron gun. As this synchronous method may not be easy to build, the present system is better to produce only accelerated particles.

An example of the experimental results showing the energy increment $\Delta\varepsilon$ vs the static magnetic field applied vertically is shown in Fig. 6. Here the energy increment of the electrons, $\Delta\varepsilon$, is defined by the difference between the accelerated energy ε and the energy without the static magnetic field, i.e., $\Delta\varepsilon \equiv \varepsilon(B) - \varepsilon(0)$. The open circles, solid circles, and solid triangles indicate the incident electron energy of $\varepsilon_{\rm in} = 60$, 62, and 64 keV, respectively. The maximum energy increment of $\Delta\varepsilon = 7.5$ keV is observed for an external magnetic field of 2.0 G. Note that a resonant interaction between the electromagnetic wave and the electrons occurs, as shown in Fig. 4, even at $B_0 = 0$. Therefore the total maximum increment of accelerated electron energy is 13.5 eV ($\Delta\varepsilon_0 + \Delta\varepsilon$) at $\varepsilon_{\rm in} =$ 62 keV. Up to about 1 G, the energy increases with increasing applied magnetic field, while above 2–2.5 G it decreases at all incident energies. These results imply that electron detrapping occurs from the wave potential above $B = 2$–2.5 G.

In Fig. 6 the calculated theoretical results are also displayed by solid lines. The calculation is performed by solving the equation of motion of an electron under the present experimental conditions. Here the Runge-Kutta method is used with 100 test particles distributed initially uniformly in the phase space. The electric field of the wave is chosen to be 20, 30, and 40 kV/m. In the figure, the solid lines show the results when the trapping condition

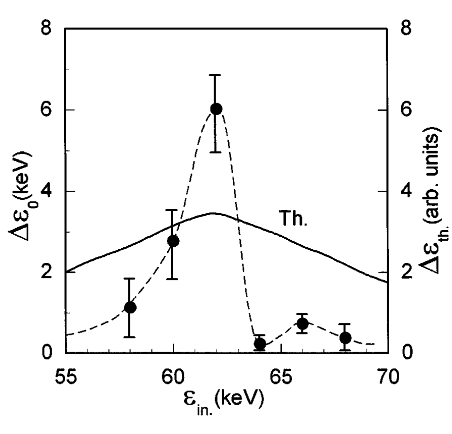

FIG. 4. Energy increment $\Delta\varepsilon_0$ as a function of the incident electron energy, $\varepsilon_{\rm in}$, without static magnetic field. Incident microwave power $P = 10$ kW. Th. shows the calculated energy increment estimated from the resonance characteristic of the slow-wave structure.

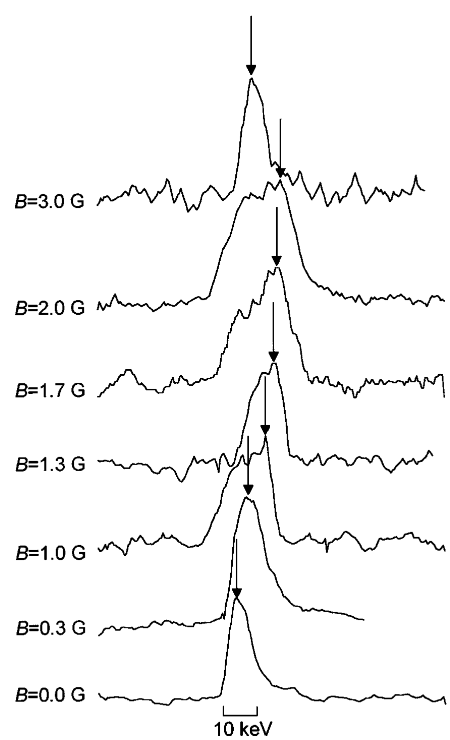

FIG. 5. Examples of the electron energy spectra at the incident electron energy of 62 keV, with $P = 10$ kW. The arrows show the peak value, the energy of which is employed.

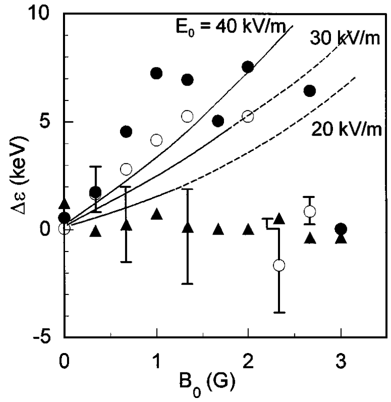

FIG. 6. Energy increment $\Delta\varepsilon$ as a function of the static magnetic field B_0 with $P = 10$ kW. The open circle stands for $\varepsilon_{\rm in} = 60$ keV, closed circle for 62 keV, and closed triangle for 64 keV. The solid lines show the calculated values for $E_0 = 20$, 30, and 40 kV/m.

is satisfied. Once Eq. (1) is violated, we cannot use the results anymore, and the dotted lines are given for comparison. The results show fairly good agreement with the experiments until detrapping occurs, although the calculated values are even smaller.

The inequality of the trapping condition [Eq. (1)] requires complete equilibrium in the phase space. In the present experiments, however, it takes about $t \geq 20$ ns to reach the steady state, while the acceleration ceases at $t < 3.6$ ns, as estimated from the time taken by the electrons to travel through the waveguide at the incident energy of 62 keV. If the saturation or decrease of the electron energy for $B \geq 2$ G is assumed to be due to the detrapping of particles from the wave trough, the detrapping time can be estimated to be about 4 ns by employing the experimental parameters ($E = 20$ kV/m, $B_0 = 2$ G, and $\varepsilon_{\rm in} = 62$ keV). The absolute value of the electric field intensity, however, cannot be measured directly. We tried to estimate it from the experimental data after fitting to the theoretical value. In Fig. 6, detrapping occurs at $B \simeq 2.5$ G for $\varepsilon_{\rm in} = 62$ keV or $B \simeq 2.0$ G for 60 keV. From Eq. (1) and the Maxwell equation, we obtain $E_0 \simeq 44$ kV/m for 62 keV and 35 kV/m for 60 keV. Now the energy gain can also be estimated with the use of Eq. (2). At $B \simeq 2.5$ G, $\Delta\varepsilon = 5.4$ keV is obtained for $\varepsilon_{\rm in} = 62$ keV, a reasonable agreement of the experimental result with the numerical calculation. Here, there is one question. In order to obtain the above-mentioned result, we employed $\Delta\varepsilon_0 = 6$ keV from Fig. 4 at $\varepsilon_{\rm in} = 62$ keV. However, for $E_0 \simeq 44$ keV, $\Delta\varepsilon_0 \simeq 0.8$ keV is expected. This discrepancy is not clarified yet. The condition of the transient state, however, should be taken into consideration for a more precise explanation of the experimental results as well as for future experiments where γ_p may be increased.

An electromagnetic wave with a different mode, such as a slow longitudinal wave (TM mode), for example, could propagate in the waveguide. In the present experimental setup, however, the results show that TM waves can propagate in the waveguide, but electrons with initial energy of 62 keV cannot interact with such waves, because of low phase velocity $(0.23c)$.

In summary, electron acceleration using a slow transverse electromagnetic wave (TE wave) supplemented with a static magnetic field has been demonstrated. A maximum energy gain of 13.5 keV for electrons is observed from an incident energy of 62 keV in a 0.5 m accelerator, when an external magnetic field of 2.5 G is applied.

Stimulating discussions with Professor S. Takeuchi are greatly appreciated. A part of the present work was supported by a Grant-in-Aid for Scientific Research from the Ministry of Education, Science and Culture of Japan, and by IDX Co., Tokyo, Japan, for machine construction.

[1] T. Tajima and J. M. Dawson, Phys. Rev. Lett. **43**, 267 (1979).
[2] C. E. Clayton, K. A. March, A. Dyson, M. Everett, A. Lal, W. P. Leemans, R. Williams, and C. Joshi, Phys. Rev. Lett. **70**, 37 (1993).
[3] J. B. Rosenzweig, D. B. Cline, B. Cole, H. Figueroa, W. Gai, R. Konecny, J. Norem, P. Schoessow, and J. Simpson, Phys. Rev. Lett. **61**, 98 (1988).
[4] H. Nakanishi, A. Enomoto, A. Ogata, K. Nakajima, D. Whittum, Y. Yoshida, T. Ueda, T. Kobayashi, H. Shibata, S. Tagawa, N. Yugami, and Y. Nishida, Nucl. Instrum. Methods Phys. Res., Sect. A **328**, 596 (1993).
[5] K. Nakajima, D. Fisher, T. Kawakubo, H. Nakanishi, A. Ogata, Y. Kato, Y. Kitagawa, R. Kodama, K. Mima, H. Shiraga, K. Suzuki, K. Yamakawa, T. Zhang, Y. Sakawa, T. Shoji, Y. Nishida, N. Yugami, M. Downer, and T. Tajima, Phys. Rev. Lett. **74**, 4428 (1995).
[6] R. Sugihara and Y. Mizuno, J. Phys. Soc. Jpn. **47**, 1290 (1979).
[7] Y. Nishida, M. Yoshizumi, and R. Sugihara, Procceedings of the 13th Annual Anomalous Absorption Conference, Banff, Alberta, Canada, 1983 (unpublished), p. F7; Phys. Lett. **105A**, 300 (1984).
[8] Y. Nishida, M. Yoshizumi, and R. Sugihara, Phys. Fluids **28**, 1574 (1985).
[9] T. Katsouleas and J. M. Dawson, Phys. Rev. Lett. **51**, 392 (1983).
[10] Y. Nishida and T. Shinozaki, Phys. Rev. Lett. **65**, 2386 (1990), and references therein.
[11] Y. Nishida and R. Sugihara, in *Laser Interaction and Related Plasma Phenomena*, edited by H. Hora and G. Miley (Plenum, New York, 1986), Vol. 7, p. 811.
[12] Y. Nishida, N. Yugami, H. Onihashi, T. Taura, and K. Otsuka, Phys. Rev. Lett. **66**, 1854 (1991); N. Yugami, H. Onihashi, K. Otsuka, T. Taura, and Y. Nishida, Japan. J. Appl. Phys. **32**, 5703 (1993), and references therein.
[13] A. Loeb and L. Friedland, Phys. Rev. A **33**, 1828 (1986).
[14] S. Takeuchi, K. Sakai, M. Matsumoto, and R. Sugihara, Phys. Lett. A **122**, 257 (1987); S. Takeuchi, K. Sakai, M. Matsumoto, and R. Sugihara, IEEE Trans. Plasma Sci. **PS-15**, 251 (1987).
[15] V. V. Apollonov, A. I. Artem'ev, Yu. L. Kalachev, A. M. Prokhorov, and M. V. Fedorov, JETP Lett. **47**, 91 (1988).